Earth Planet. Sci. Lett. 627 (2024) 118561

Contents lists available at ScienceDirect

Earth and Planetary Science Letters

journal homepage: www.elsevier.com/locate/epsl

Lesser Antilles slab reconstruction reveals lateral slab transport under the Caribbean since 50 Ma

Yi-Wei Chen [a,b,*], Jonny Wu [a,d], Saskia Goes [c]

[a] Department of Earth and Atmospheric Science, University of Houston, Houston, TX
[b] Deaprtment of Astronomical and Physical Geodesy, Technical University of Munich, Munich, Germany
[c] Department of Earth Science & Engineering, Imperial College London, London
[d] Department of Geosciences, University of Arizona, Tucson, AZ

ARTICLE INFO

Editor: Dr H Thybo

Keywords:
slab dragging
vertical slab sinking
Proto-Caribbean

ABSTRACT

The link between surface tectonic plates and mantle slabs is fundamental for paleo-tectonic reconstructions and for our understanding of mantle dynamics. Many seismic tomography-based studies have assumed vertical slab sinking and projected mantle features to the surface to reconstruct paleo-trench locations or explain tectonic features. Here, we used a slab-unfolding approach that does not require assumptions about sinking paths or rates to re-interpret the seismic structure of the Lesser Antilles slab underneath the Caribbean. A recent study invoked mainly vertical slab sinking and a highly folded and deformed slab to explain seismic Caribbean mantle structures. However, our results show that the upper-mantle Lesser Antilles slab structure can be better explained by limited intra-slab deformation and up to ~900 km lateral slab transport towards the northwest after subduction. Our results indicate that such lateral slab transport can occur even with probable weaknesses in the slab that originate from a subducted fossil ridge-transform system. We ascribe the lateral slab transport in the mantle to a kinematic connection with the North American plate, which has migrated northwestward since the Eocene.

1. Introduction

The current locations of tomographically-imaged slabs (i.e., subducted oceanic lithosphere) within the mantle have often been used to reconstruct their ancient sites of subduction (Braszus et al., 2021; Chen et al., 2019; Ren et al., 2007; van Benthem et al., 2013; van der Hilst et al., 1997; van der Meer et al., 2018; Wu et al., 2016) and can be used to infer sinking trajectories of subducted slabs in the mantle (Braszus et al., 2021; Chertova et al., 2014; Parsons et al., 2021; Sigloch and Mihalynuk, 2013; Spakman et al., 2018; van de Lagemaat et al., 2018; van der Meer et al., 2018). Some studies imply or assume that slabs will predominantly sink vertically into the mantle, i.e., the vertically sinking slab end-member (Braszus et al., 2021; Ren et al., 2007; Sigloch and Mihalynuk, 2013; van der Meer et al., 2018). In contrast, other studies argue that some subducted slabs are dragged and transported laterally, possibly by as much as >1000 km, within the mantle after subduction, i.e., the lateral slab transport end-member (Chertova et al., 2014; Parsons et al., 2021; Peng and Liu, 2022; Spakman et al., 2018; van de Lagemaat et al., 2018), which would be inconsistent with vertical slab sinking assumptions. These distinctions are important because they would lead to different and possibly erroneous predictions for paleo-trench locations in plate reconstructions that could have wide-ranging tectonic implications, for example, for terrane accretion histories along western North America (Pavlis et al., 2019; Sigloch and Mihalynuk, 2013, 2017). The paths of subducted slabs within the mantle also provide important inputs or tests for mantle circulation models (e.g., Peng and Liu, 2022).

For the Caribbean region (Fig. 1), studies have proposed contrasting interpretations, where either subducting slabs are laterally-mobile while sinking in the mantle (e.g., Fraters et al., 2019) or sink mainly vertically (e.g., Braszus et al., 2021). Braszus et al. (2021) revised the regional plate reconstruction of the Caribbean since the Late Cretaceous and reconstructed spreading ridge segments within the now-subducted Proto-Caribbean/Atlantic oceanic lithosphere (i.e., Lesser Antilles slab). Braszus et al. (2021) showed that a simple, vertical projection provided the best fit between their reconstructed Proto-Caribbean spreading ridge segments and slower seismic velocity anomalies within the slab in their tomography model, VoiLA-P19 (black circles in Fig. 2), implying a dominant vertical sinking and significant folding of the Lesser Antilles slab during the past 100–120 Myr of subduction. In contrast, Fraters et al. (2019) and Fraters (2019) show in a geodynamic

* Corresponding author.
E-mail address: yiweichen.tw@gmail.com (Y.-W. Chen).

https://doi.org/10.1016/j.epsl.2023.118561
Received 2 June 2023; Received in revised form 2 November 2023; Accepted 24 December 2023
Available online 8 January 2024

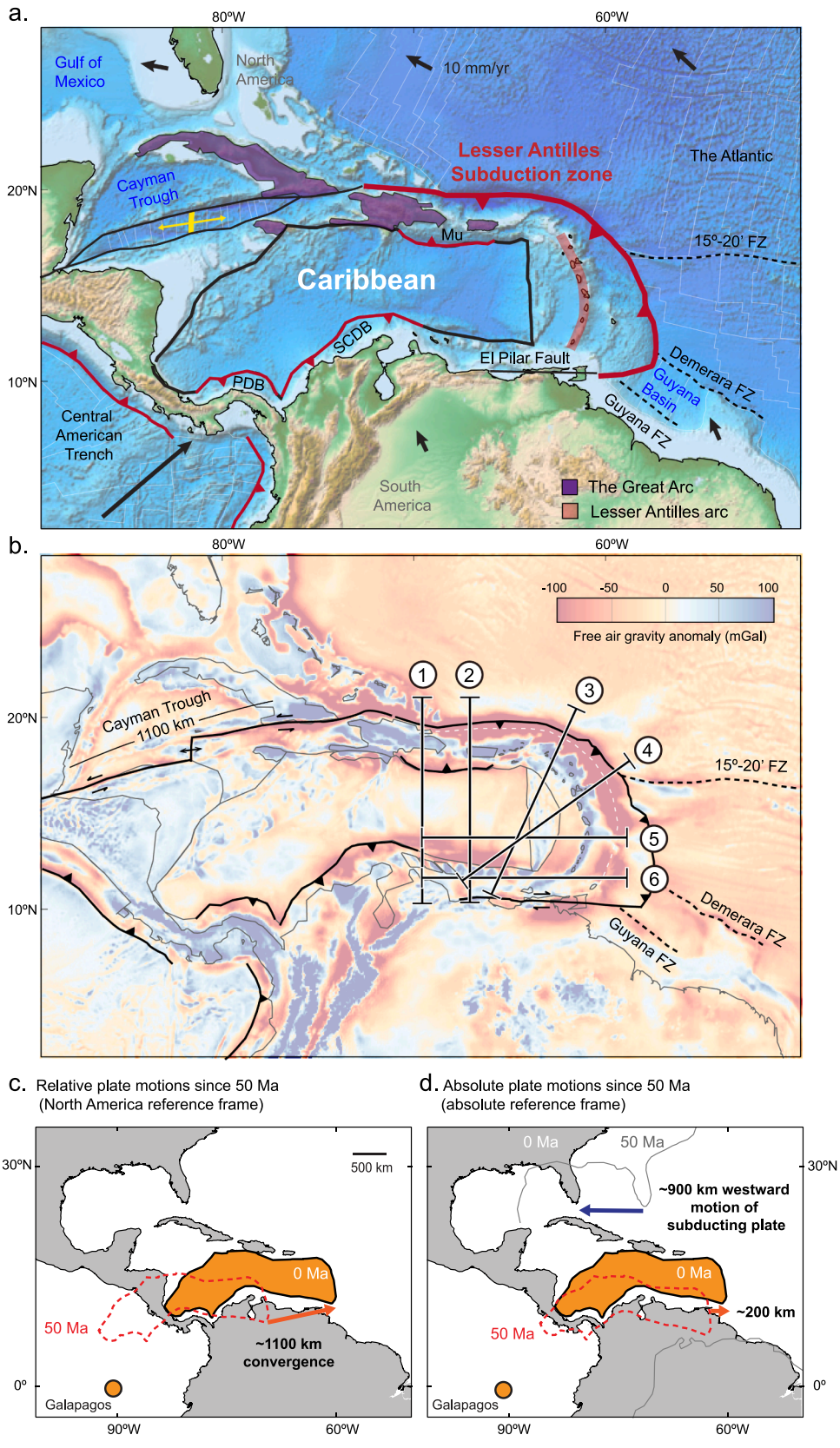

(caption on next page)

Fig. 1. Caribbean tectonic map. (a) Current plate boundaries of the Caribbean (Bird, 2003). The Lesser Antilles subduction front is highlighted with a bold red line. Other subduction zones are shown as thin red lines with teeth. Strike-slip plate boundaries are shown as black lines. The dashed black line marks the 15°20′ Fracture Zone (15°20′ FZ), which is probably the current plate boundary between the North and South Atlantic. Plate velocities (black arrows) are from Müller et al. (2019). Mu: Muertos Trough; PDB: Panama Deformation Belt; SCDB: South Caribbean Deformation Belt. (b) Satellite-derived free-air gravity anomalies (Sandwell et al., 2014) reflect tectonic features on the subducting Atlantic plates. Major oceanic fracture zones are marked with dotted black lines. The white dashed line follows the gravity low near the subduction zone, possibly indicating the bending location of the subducting plate. The location of the seismic tomography cross-sections in Fig. 3 is shown and labelled by circled numbers 1 to 6. (c) and (d) are the Caribbean-North American plate convergence since 50 Ma. (c) In a North American fixed reference frame, the total convergence since 50 Ma is around 1100 km and the relative motion of the Caribbean plate is eastwards. However, (d) an absolute reference frame (Müller et al., 2019) shows that the Caribbean plate is nearly stationary, and the west-moving and subducting North American plate contributes most of the plate convergence.

model that, for their preferred set of plate and mantle rheological parameters, the relatively old and slowly subducting Lesser Antilles slab can be laterally transported and sheared by the westward-moving North American plate. To further explore these contrasting results, in this study, we used a slab unfolding approach to restore the Lesser Antilles slab back to the Earth's surface and reevaluate the tectonic evolution of the Caribbean since the early Cenozoic.

2. Regional geology

The present-day Caribbean plate is bounded by two inward-dipping subduction systems on its eastern (Lesser Antilles) and western (Central America) margins (Fig. 1a). The core of the present-day Caribbean plate has been interpreted as the Caribbean large igneous province (CLIP) that erupted material with ocean-island-basalt (OIB) geochemical signatures (Whattam and Stern, 2015) when positioned near the Galapagos hotspot in the eastern Pacific Ocean. The main phase of the eruption occurred in the Coniacian-Santonian (~100 to ~85 Ma) (Whattam and Stern, 2015).

The Great Arc of the Caribbean (GAC), at the eastern edge of the CLIP, consumed the Mesozoic Proto-Caribbean ocean basin (150–65 Ma) that originally occupied the space between the Americas (Pindell and Kennan, 2009). In the mid-Eocene (~50 Ma), a regional plate reorganization occurred (Pindell and Kennan, 2009). Convergence along the northwestern Cuban section of the Greater Arc ceased as the arc docked to the North American margin (Pindell et al., 2005; Pindell and Kennan, 2009), while subduction activity continued in the east, jumping to the (Outer) Lesser Antilles Arc (Fig. 1a) (Allen et al., 2019). In response to this reorganization, a new strike-slip plate boundary formed within the Caribbean, opening the Cayman Trough (Fig. 1a), from 49.6 Ma, as a pull-apart basin (Mann et al., 2006). The ~1100 km-long Cayman Trough recorded the relative plate motion between the overriding Caribbean and the subducting Atlantic since the Eocene (Fig. 1c); in other words, the kinematics of Cayman Trough opening robustly constrains ~1100 km of Atlantic subduction beneath the Caribbean plate along the Lesser Antilles subduction zone. Additional plate convergence of 250–500 km is possible if more complicated intra-plate deformation from tectonic rotations is considered (see Discussion in 5.1) (Montheil et al., 2023). To the south, the El Pilar strike-slip fault system (Fig. 1a) forms the South America-Caribbean boundary, serving as a STEP-fault plate boundary (Subduction-Transform-Edge-Propagator) (Govers and Wortel, 2005).

3. Method

3.1. Mantle tomography underneath the Caribbean

The mantle structure under the eastern Caribbean has been widely investigated by using seismic tomography (Bezada et al., 2010; Braszus et al., 2021; Harris et al., 2018; Miller et al., 2009; van Benthem et al., 2013; VanDecar et al., 2003). In this study, we show three widely-used and recently published mantle tomography models side-by-side, including VoiLA-P19 (Braszus et al., 2021), UUP07 (Amaru, 2007), and HP2018 (Harris et al., 2018) (Figs. 2 & 3). The orientation of the vertical cross sections (Fig. 1b) is intended to be perpendicular to the current subduction front.

The VoiLA-P19 model (Braszus et al., 2021) is the most recent regional P-wave travel-time tomographic model that includes, in addition to a global travel time data set, seismic data from the temporary broadband ocean-bottom seismometers (OBS) deployment from the VoiLA experiment (Goes et al., 2019). The UUP07 model (Amaru, 2007) is a global P-wave travel-time tomography with a variable horizontal resolution, and the best-resolved parts within our study region have a lateral resolution of about 150–200 km in the upper mantle and 200–300 km in the lower mantle (van Benthem et al., 2013). The HP2018 model (Harris et al., 2018) is a regional P-wave tomography based on finite frequency kernels and teleseismic P and PP travel-time residuals. We masked the areas that Braszus et al. (2021) identified as poorly resolved in transparent white, and we overlayed these same areas over the other models where these regions are probably also poorly sampled (Fig. 3), although we acknowledge that resolution will differ between the models.

3.2. Slab mapping and unfolding

Using the software Gocad, we manually mapped the mid-slab surface in the UUP07 model in 3D (Fig. 4a) based on seismicity and relatively fast velocity perturbation anomalies in the tomographic models. We then transferred the seismic velocity onto the mapped slab (Fig. 4c) to facilitate visualizing the seismic character of the slab. Following Wu et al. (2016), we flexurally unfolded (i.e., structurally restored) the mapped slab (Fig. 4d) back to its original position at the surface, minimizing surface area and internal deformation of the plate.

We then input the unfolded slabs into a paleo-GIS (geographic information system) software, GPlates (Boyden et al., 2011). Assigning the plate motions of the parent plate (i.e., the North America plate) from Müller et al. (2019) to the unfolded slabs (Fig. 4d), we "unsubduct" the slab back to the late Cretaceous (Fig. 6). We chose the North American plate as the parent plate because the Lesser Antilles slab is apparently detached from South America along the El Pilar strike-slip fault system (Fig. 1a). For illustration, several reference frames are used in subsequent figures. The choice of reference does not affect the relative motion between surface plates, best illustrated in a South American-fixed reference frame (Fig. 6), while an absolute (mantle) reference frame (Figs 8 & 9) better illuminates the relative motion between plates and mantle slabs.

4. Results

4.1. Comparison of slab tomographic anomalies

To a first order, the three tomography models show similar slab-like, fast velocity anomalies for the Lesser Antilles slab that at depths < 250 km coincide with its Benioff zone seismicity (Fig. 2). The black dashed lines in Figs. 2 and 3 show that all three tomographic models image the center of the slab anomaly (i.e., mid-slab) at similar locations. Braszus et al. (2021) interpreted lower-wavespeed anomalies within the Lesser Antilles slab imaged in VoiLA-P19 as subducted (fossil) spreading ridges (black circles in Figs.2a to d) and tears along subducted fracture zones (red arrows in Figs.2a to d). Our comparison of all three tomographic models confirms that these lower-wavespeed features can be seen in all

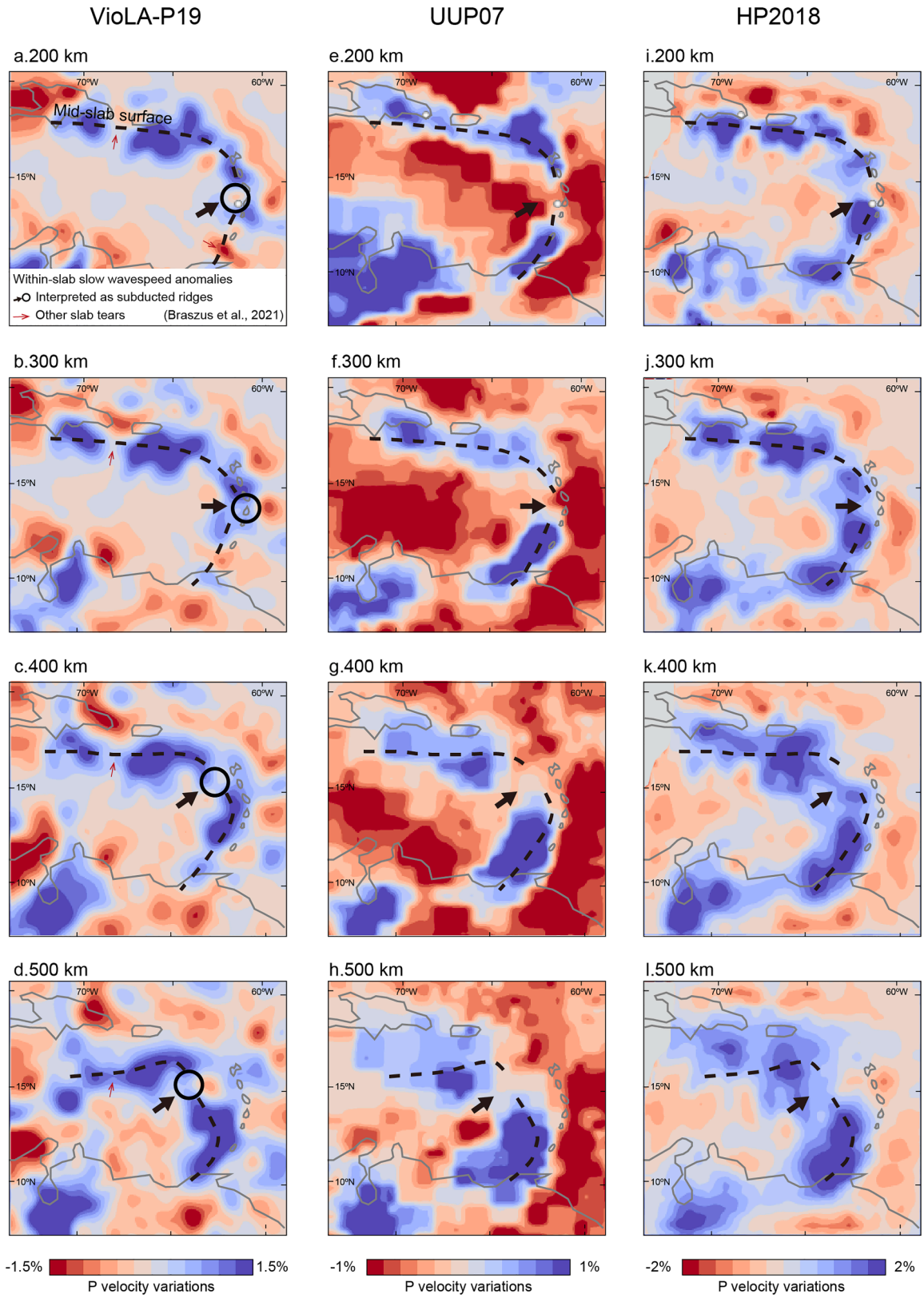

Fig. 2. Comparison of three tomographic models for the Caribbean mantle structure. Map views of horizontal depth sections through three tomographic models: VoiLA-P19 (Braszus et al., 2021), UUP07 (Amaru, 2007), and HP2018 (Harris et al., 2018). White dots mark the hypocentres of Wadati-Benioff zone seismicity (Engdahl and Villaseñor, 2002). The dashed black lines follow our mapped mid-slab surface from the VoiLA-P19 model, and these are also shown on the other two tomographic models for comparison. Open circles are locations of the slow wavespeed anomalies within the slab that were interpreted as subducted spreading ridges by Braszus et al. (2021). The locations of these anomalies are generally consistent with the other two models (black arrows). Red arrows mark the anomalies interpreted as slab tears along former fracture zones (Braszus et al., 2021).

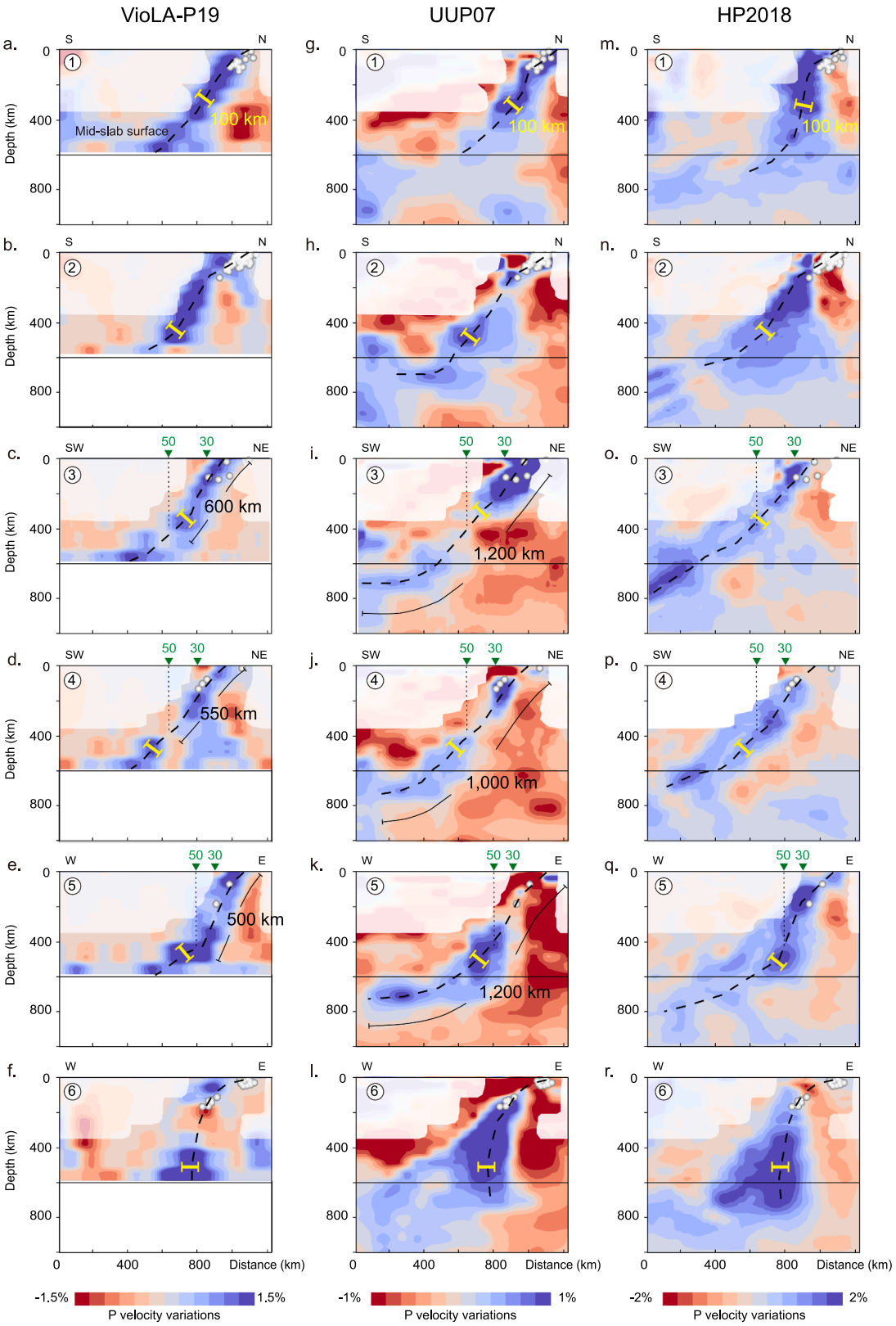

Fig. 3. Vertical tomographic cross-sections of the three tomography models VoiLA-P19 (Braszus et al., 2021), UUP07 (Amaru, 2007), and HP2018 (Harris et al., 2018). The cross-section locations are shown in Fig. 1b. Structures are masked in transparent white where resolution is limited according to Braszus et al. (2021). White dots mark Wadati-Benioff zone seismicity. The black dashed lines follow the mid-slab surface of the Lesser Antilles slab for each of the models. Green upside-down triangles mark the reconstructed Lesser Antilles paleo-trench locations from this study at 50 Ma and 30 Ma, respectively. Yellow bars indicate a reference thickness of 100 km. The 50 Ma trenches are vertically projected (black dotted lines) onto the slab, from which the lengths are measured along the slab to the present trench, as shown in the left column. The total slab lengths are also measured and shown in the middle column.

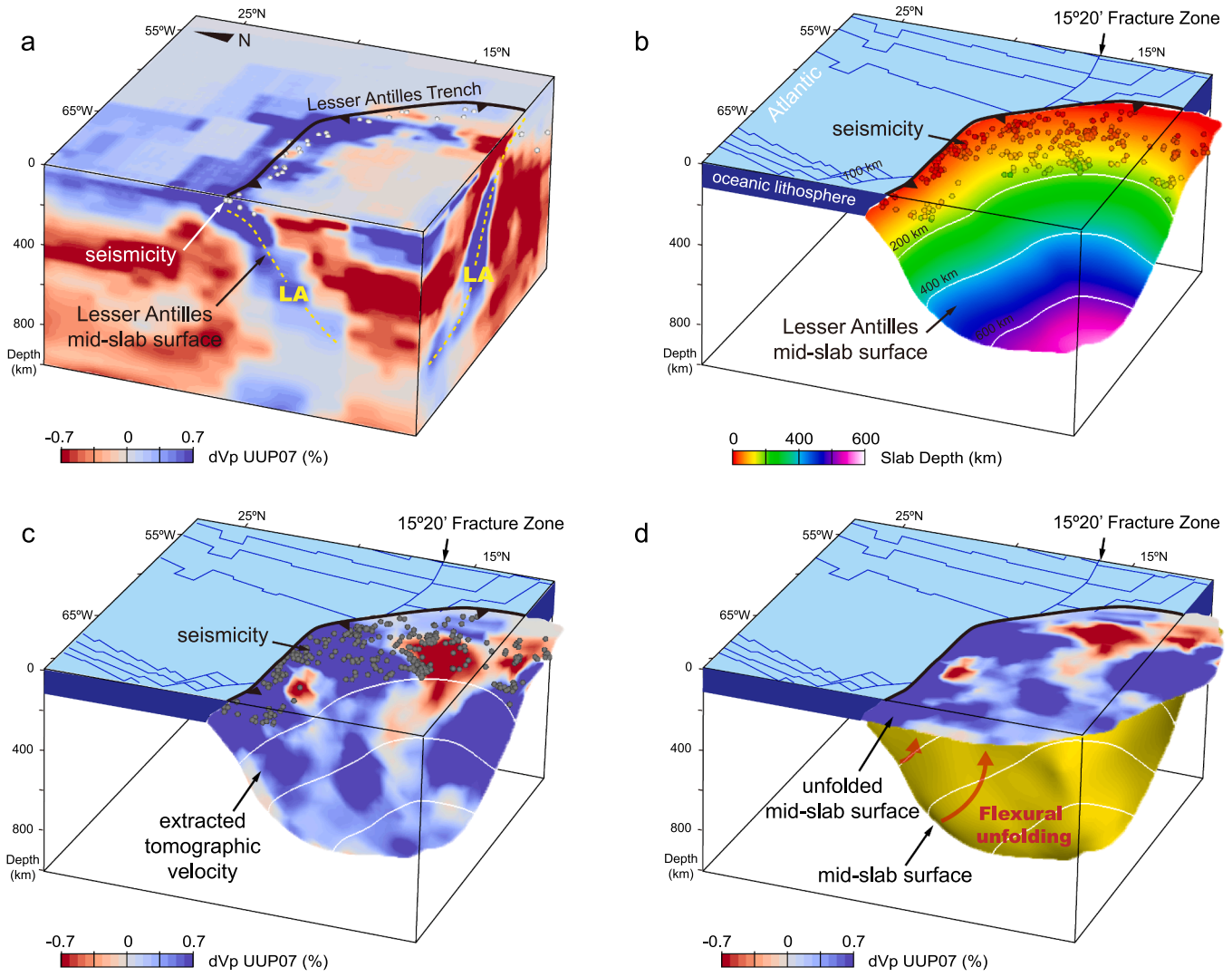

Fig. 4. Slab unfolding workflow. (a) Lesser Antilles (LA) mid-slab surface (yellow dashed lines) mapped in 3D on model UUP07 (Amaru 2007). White dots are seismicity from the CMT catalog (Dziewonski et al., 1981; Ekström et al., 2012) and Bie et al. (2019). (b) 3D slab geometry. Seismicity is color coded with depth. Blue lines on the top surface follow Atlantic seafloor isochrons (Müller et al., 2019) (c) The wavespeeds (seismic velocity) of UUP07 as measured along the inferred mid-slab surface. Seismicity (same as b) is shown as gray dots. (d) Slab after flexural unfolding following the approach of Wu et al. (2016), with mid-slab wavespeeds.

models (black arrows Fig. 2). East-west cross sections show that the Lesser Antilles slab dip is ~45° in the mid-upper mantle and exhibits a shallower dip within the mantle transition zone and uppermost lower mantle down to ~800 km depth, except for the southernmost cross section (6), where the slab is steeply-dipping and terminates near 800 km depth (Fig. 3). Both the UUP07 and HP2018 tomographic images extend into the lower mantle and (assuming no significant buckling) show the Lesser Antilles slab length is about ~1100 km-long (Fig.3, and also Fig. 5 in van Benthem et al. (2013))

The VoiLA-P19 model (Braszus et al., 2021) shows the most uniform slab thickness with no clear indication of significant slab thickening/folding with depth (Fig. 3), except in Section 6 (Fig. 3f), where apparent thickening is found in all three models. Such apparent thickening might be the result of an oblique cut through a slab that bends east-west wards (Bezada et al., 2010; Braszus et al., 2021; Harris et al., 2018; Miller et al., 2009; van Benthem et al., 2013) near the South American margin. As Section 6 is neither perpendicular to the arc (Fig. 1a) nor to the gravity low (white dashed line in Fig. 1b), the section might also not be perpendicular to the slab at depth. Alternatively, a more complicated slab structure with detached South American continental lithosphere (Levander et al., 2014; Miller et al., 2009) has been proposed at South America- Caribbean boundary, which might account for the thickening.

4.2. Slow wavespeed anomalies within the slab

Our mapped Lesser Antilles slab with the transferred wavespeeds from the UUP07 model shows several patches of reduced (i.e., slower) P-wavespeed anomalies on the slab. The three most prominent features are under Puerto Rico (the northern anomaly, AN in Fig. 5a), the central Antilles (A0 in Fig. 5a), and Grenada (the southern anomaly, AS in Fig. 5a). Independent geophysical observables also show distinct observations at these locations (Figs. 5b & c), supporting that they are not artifacts, but indeed features distinct from the rest of the slab.

Near A0, between 13.5°N to 14.5°N, intermediate-depth seismicity (70–300 km) is significantly less (Fig. 5b). Slightly north of A0, between 14.5°N to 15.5°N, the majority of strong (Mw>4.0) deep earthquakes (150 km depth) along the Lesser Antilles Arc was found (Lindner et al., 2023). Near A0 and AN, the focal mechanisms of these intermediate-depth earthquakes reflect trench-parallel extension (Bie et al., 2019; Lindner et al., 2023) (Fig. 5b), which is distinct from the rest of the slab that shows mainly trench-perpendicular compression or extension (Bie et al., 2019; see Lindner et al., 2023 for more comprehensive comparison). A recent stress inversion study confirms

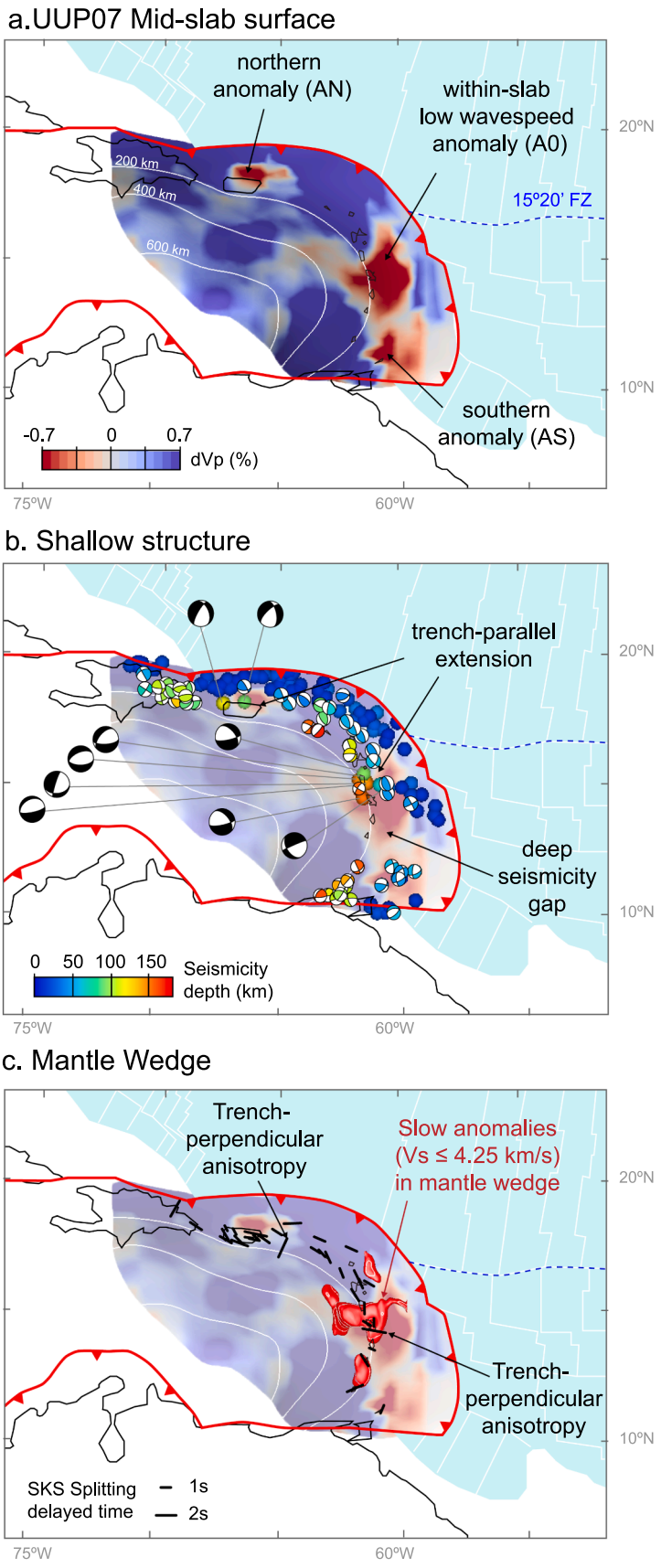

(caption on next page)

Fig. 5. Interpreted within-slab slow wavespeed anomalies in the present-day geometry of the subducted Lesser Antilles slab, in map view. (a) Mid-slab surface mapped from UUP07 with labeled slow wavespeed anomalies. (b) Comparison of mid-slab wavespeed structure from (a) to the locations of Wadati-Benioff zone earthquakes from the CMT catalog (Dziewonski et al., 1981; Ekström et al., 2012) that are color-coded with depth. Only the seismicity around the slab (within 50 m above the mid-slab surface) is shown. The focal mechanism solutions between 50 and 300 km depth from the CMT catalog (Dziewonski et al., 1981; Ekström et al., 2012) are shown and color-coded with depth. We highlighted the solutions in black that show trench-parallel extension near the slow wavespeed anomalies in (a). (c) Comparison of slow anomalies within the mantle wedge above the slab (red bodies) to seismic anisotropy from the shear-wave splitting where black lines reflect the fast wavespeed directions and splitting magnitude (Schlaphorst et al., 2017). The red bodies are slow wavespeed body (Vs $\leq$ 4.25 km/s) in the mantle wedge from the Rayleigh wave tomography of Harmon et al. (2021).

slab-parallel extension near A0 underneath Dominica (Lindner et al., 2023). Imaged patterns in teleseismic shear wave splitting (SKS) show trench-perpendicular anisotropy near A0 (Schlaphorst et al., 2017) and AN (Meighan and Pulliam, 2013) (Fig. 5c), which are different from the overall trench-parallel anisotropy found along the rest of the slab (Fig. 5c). In a Rayleigh wave tomographic study (Harmon et al., 2021), an anomalous slow wavespeed mantle wedge was found above the slab, extending 200 km into the backarc (isosurface shown as a red body in Fig. 5c), which was interpreted as a particularly hydrous/melt-rich mantle wedge fed by dehydration of tectonic features in the subducting plate. The location of the anomalously slow mantle wedge overlies our mapped A0. We, therefore, conclude that these three slow wavespeed anomalies are real features within the Lesser Antilles slab. There are a few other low-velocity anomalies in the deeper slab (A1 and A2 in Fig. 6e; supplementary Figure 1; discussed below), which are also seen in all models, and may thus also reflect structures inside the subducted slab.

Although the locations of these anomalies are consistent between the different studies, we note here that the interpretation of absolute wavespeed of these features requires caution. Compared to the other two regional tomography (Fig. 2; Supplementary Fig. 1), the anomalies in UUP07 model have slower wavespeeds, which could be affected by more smearing of the anomalies from the slow mantle wedge above (Fig. 5c). The UUP07 model has good large-scale coverage, but less regional data coverage than the two more recent models.

What causes these features within the slab remains debated. For example, A0 anomaly has been interpreted as a slab gap (Schlaphorst et al., 2017), torn along the subducted Equatorial–Atlantic transform boundary (which is probably currently close to the 15°20′ Fracture Zone in Fig. 1a) (Braszus et al., 2021; van Benthem et al., 2013). Alternatively, the A0 anomaly has been interpreted as a particularly hydrated section of the subducted lithosphere, possibly near the subducted spreading center (Braszus et al., 2021). In the next section, we will explore the possible cause of these anomalies through a plate reconstruction.

4.3. Inferred ridge-transform system

To better understand the potential causes of these wavespeed anomalies on the slab, we embedded our unfolded (i.e., structurally-restored) slab (Fig. 6a) into a quantitative global plate reconstruction in a South-America fixed reference frame (Fig. 6), similar to other regional plate reconstructions (e.g., Mann et al., 2006; Pindell and Kennan, 2009). When restoring the unfolded Lesser Antilles slab (Fig. 6a) back to ~50 Ma, the ~1100 km-long unfolded slab fills the gap between the reconstructed trench position at the front of the overriding Caribbean at that time and the currently unsubducted Atlantic lithosphere (Fig. 6d).

The tectonic meaning of the wavespeed anomalies is proposed based on our reconstructed age structure of the Proto-Caribbean seafloor in the late Cretaceous, the time that the spreading between North and South America ceased (Müller et al., 2019). At 70 Ma (Fig. 6e), we found that anomaly A0 reconstructs close to the ridge-ridge-ridge triple junction with the North and South Atlantic spreading ridges. We, therefore, interpret the reduced wavespeed anomaly, A0, as one arm of this triple junction system (Fig. 6e), and associate it with an easternmost segment of the Proto-Caribbean ridge, R0. When compared with the published sea floor ages on the Lesser Antilles slab (Fig. 6f) inferred from the separation history between the North and South America (Braszus et al., 2021), we found that their proposed ridge segments R1 and R2 collocated with two other slow wavespeed zones on our unfolded slab, which we labeled as A1 and A2 in Fig.6e. We, therefore, interpret these anomalies as the signatures of this subducted segmented spreading ridge (Fig. 6e) offset by fracture zones. These ridge segments would have been fossil ridges because Proto-Caribbean spreading ceased ~10 Ma before the subduction of R2.

We extended the Demerara and Guyana fracture zones onto our unfolded slab, as shown in black dotted lines (Fig.6e). In this study, we slightly updated the location of the Guyana fracture zone (called FZ1 in Braszus et al., 2021) based on a recent seismic reflection study (Trude et al., 2022). Braszus et al. (2021) already interpreted the anomaly we named AS as the expression of a tear along the Guyana fracture zone. This is consistent with the fact that we find that the locations of AS and AN coincide with the position of two extrapolated fracture zones (Fig. 6e), and we interpret both as expressions of fossil fracture zones.

We confirm the conclusions of Braszus et al. (2021) that the wavespeed anomalies and edges of the Lesser Antilles slab follow pre-existing spreading ridges and fracture zones. However, there are two key differences between our proposed ridge-transform system (Fig. 6e) and the one proposed previously (Fig. 6f) (Braszus et al., 2021). First, we propose an additional ridge segment, R0, based on the A0 slow wavespeed zone on the slab (Fig. 6e). Secondly, we found that the southwestern edge of our unfolded Lesser Antilles slab is roughly parallel to the two fracture zones, and we interpret the southwestern edge of our unfolded slab as coincident with another subducted fracture zone, which we named the Caracas fracture zone (Fig. 6e). Our proposed fracture zone location (at ~65°W today) is close to FZ2 from Braszus et al. (2021), but adjusted so that it roughly aligns with an important boundary on the South American continent that defines different extensional regimes (Fig. 6e). To the west, the crust is highly stretched with many extensional basins (Cediel, 2019) and has a thin lithospheric mantle (Masy et al., 2015) whereas, to the east, both the crust (Schmitz et al., 2021) and the lithospheric mantle (Masy et al., 2015) are less stretched. Different extensional regimes separated by fracture zones/ transfer zones in the adjacent continental margin are also found in other extensional margins (e.g., Brune et al., 2014). Our proposed configuration leads to more even spacing between transform faults of around 350 km along the intersecting mid-ocean ridges (Fig. 6e), which is similar to the spacing of transform faults in the Atlantic (400 $\pm$ 200 km) (Macdonald, 1998). A 3D summary of our interpretations of these wavespeed anomalies on the slab is shown in Fig. 7.

4.4. Unfolded-slab plate reconstruction

The time evolution of our unfolded-slab plate reconstruction shows that subduction of our 1100 km unfolded Lesser Antilles slab began in the Eocene (Fig. 6d). This is consistent with the 1100 km convergence between the Caribbean and the North America plate constrained by the magnetic anomalies in the Cayman trough (Fig. 1a). The start of subduction of our unfolded Lesser Antilles slab coincides with the time of the arc jump from the Aves Ridge/Greater Arc (Fig. 6d) to the (Outer) Lesser Antilles arc in the Eocene which opened the back-arc Grenada Basin (Allen et al., 2019). The three ridge segments R2, R1, and R0 were subducted at 50 Ma (Fig.6d), 30 Ma (Fig. 6c), and 10 Ma (Fig. 6b), respectively.

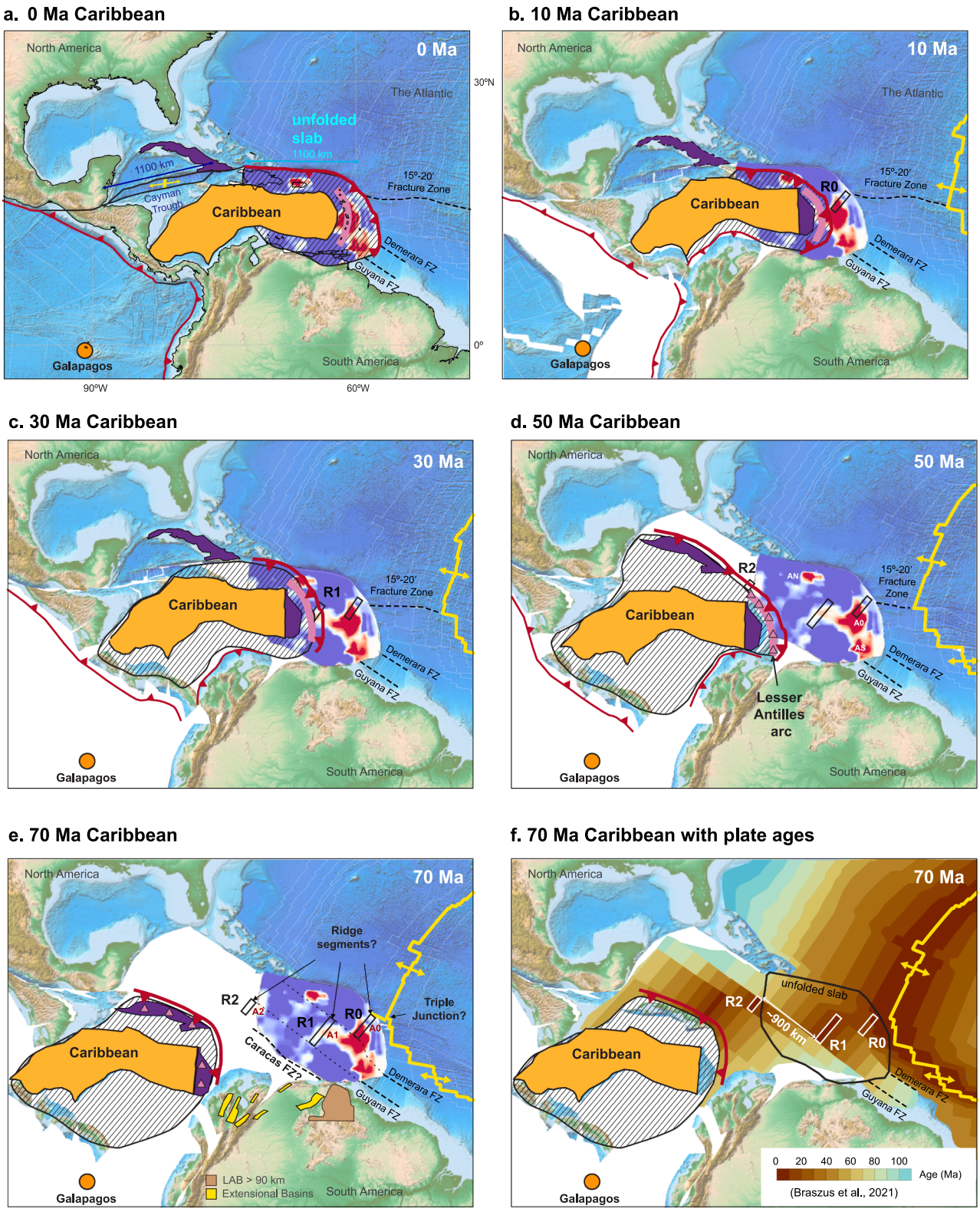

Fig. 6. Plate reconstruction map views of our unfolded Lesser Antilles slab for the past 70 Ma. (a) The unfolded slab at 0 Ma. Present-day existing fracture zones are shown as black dashed lines. The location of the Guyana fracture zone is after Trude et al. (2022). White lines are magnetic isochrons from Müller et al. (2019). We used a South American fixed reference frame in our reconstruction (see Fig. 1d for a mantle reference frame). (b) The unfolded slab at 10 Ma, following the global plate reconstruction of Müller et al. (2019). Spreading ridges are shown as yellow lines. (c) The unfolded slab at 30 Ma, (d) 50 Ma, and (e) 70 Ma, respectively. On (e), yellow polygons on (e) are extensional basins (Cediel, 2019), and brown polygons mark regions with a thick lithospheric mantle (i.e., lithosphere-asthenosphere boundary LAB deeper than 90 km) (Masy et al., 2015). (f) The 70 Ma seafloor ages from Braszus et al. (2021). Our interpreted ridge segments, R0, R1, and R2 are shown as black boxes. The dotted black lines show the extended fracture zones. According to the reconstruction, ridge segments R1 and R2 were subducted at 50 Ma and 30 Ma, respectively.

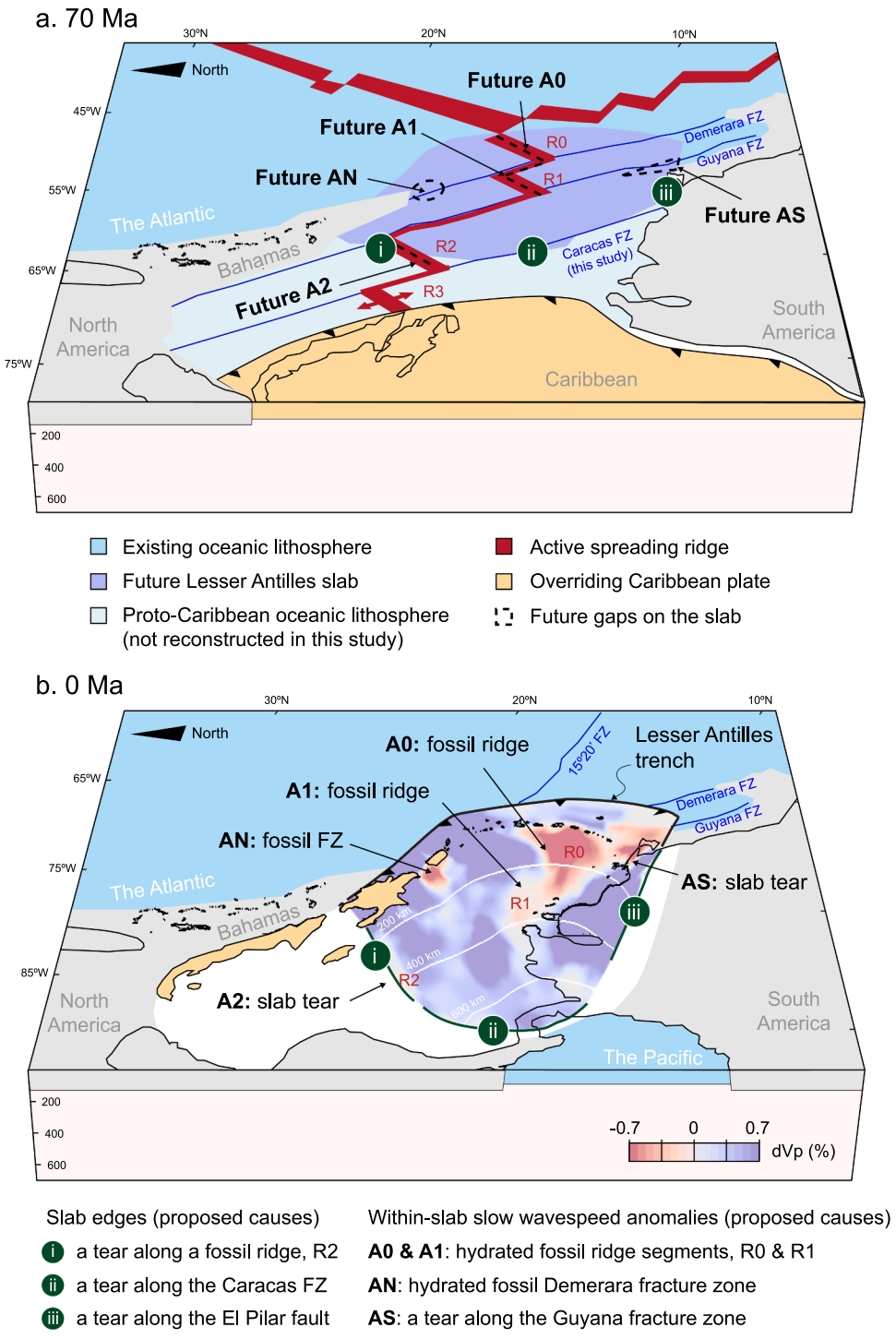

Fig. 7. Pre-existing weak zones influence the fragmentation of the Lesser Antilles slab. (a) Plate reconstruction that shows our interpretation that the present-day slab edges and the within-slab slow wavespeed anomalies represent subducted, and probably still weak, plate boundaries from 70 Ma. Fracture zones are shown in blue and spreading ridges are shown in red. Future wavespeed anomalies and tears are highlighted in black dashed lines. (b) Present day Lesser Antilles slab with transferred wavespeeds from the UUP07 seismic tomography. Our interpreted causes of the slab edges and the within-slab slow wavespeed anomalies are labeled.

The post-Eocene subduction history is kinematically-robust because the overriding Caribbean plate is connected to the subducting Atlantic via the plate circuit after the Eocene due to the Cayman Trough opening (Fig. 1a) (Müller et al., 2019). Although such convergence is usually portrayed as a result of the east-moving Caribbean plate in a fixed American reference frame (Fig. 2c), in an absolute (i.e., mantle) reference (Müller et al., 2019), the westwards-moving North American and South American plates contribute most of the convergence under the eastern margin of a near-stationary overriding Caribbean plate (Fig. 2d). Such a stationary Caribbean plate is a robust output from all tested mantle references (Müller et al., 1993; Müller et al., 2019; Torsvik et al., 2019).

5. Discussion

5.1. Inferred mantle dynamics of lateral slab transport after subduction

We estimate the degree of lateral slab transport after subduction using our reconstructed spreading ridges R2, R1, and R0 as reference points. To do this, we compare the present locations of the subducted spreading ridges (Fig. 8a; Supplementary Fig. 1) against their reconstructed subduction locations along the Lesser Antilles paleo-trench (Figs. 8b, c; Supplementary Fig. 1). The now-subducted spreading ridge R2 is currently under southern Hispaniola (i.e., A2 in Fig. 8a) but was initially subducted ~900 km ESE of its present location (black dot in Fig. 8b) at 50 Ma based on our plate reconstruction (Fig. 6d). Similarly, the now-subducted spreading ridge R1 is currently at 15°N latitude and SE of Puerto Rico (i.e., A1 in Fig. 8e) but was subducted ~350 km southeast of its present location (black dot in Fig. 8c) at 30 Ma, based on our plate reconstruction (Fig. 6c). A 3D visualization of the offset subducted ridges R2 and R1 is shown in Fig. 8d.

Our reconstructed ~900 km lateral offset between the 50 Ma and 0 Ma R2 locations cannot be explained by purely vertical slab sinking, which would cause a subducted feature to remain in the same lateral position over time. There is a similarly oriented but smaller (~350 km) offset between the 30 Ma and present 0 Ma location of the subducted spreading ridge R1 (Fig. 8c), which suggests that the lateral slab

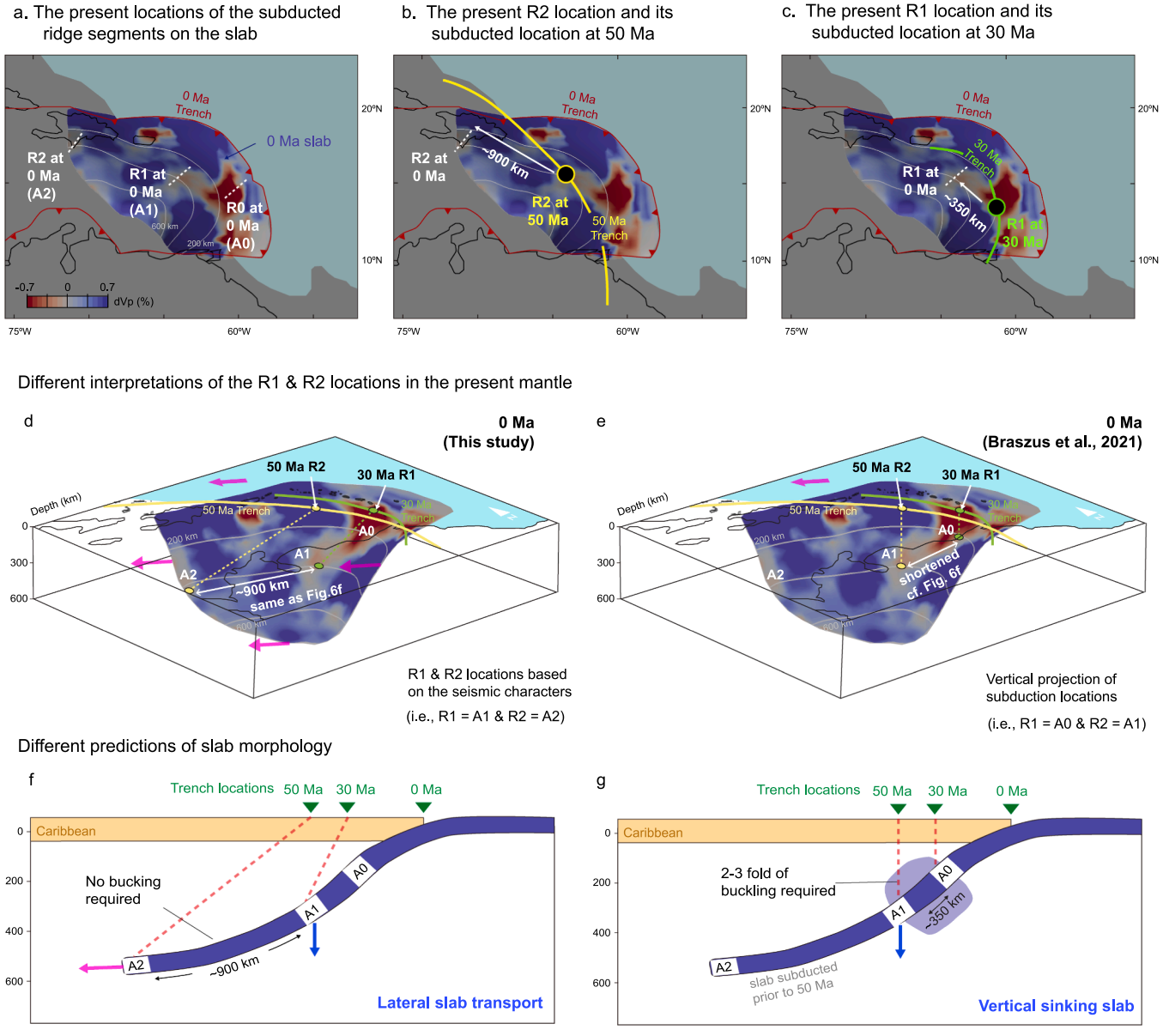

Fig. 8. Comparison between the present and past locations of subducted seafloor spreading ridges R2, R1 and R0. (a) Map of the present locations of the three subducted Proto-Caribbean ridge segments R0, R1, and R2 on the Lesser Antilles slab as inferred from interpreting the tomographic wavespeed anomalies A0, A1, A2. Comparison between the (b) present (i.e., A2) and 50 Ma location of R2 and (c) present (i.e., A1) and 30 Ma location of R1 indicates ~900 km and ~350 km offsets, respectively. We interpret these offsets to as the result of lateral slab transport after subduction. (d) & (e) Comparison between our interpretation of a laterally mobile Lesser Antilles slab with a previous interpretation (Braszus et al., 2021) that assumes vertical slab sinking. Both models agree on the subduction locations of R2 and R1 along the Lesser Antilles paleo-trench at 50 Ma (yellow line) and 30 Ma (green line); however, there are different interpretations of the present-day R1 and R2 locations on the Lesser Antilles slab. (f) and (g) show different predictions of slab morphology. In a vertical sinking slab scenario, the separation of A0 and A1 is only 350 km in the present mantle, compared to the original separation of R1 and R2 (~900 km) in the reconstruction in Fig. 6e. 2–3 folds of slab buckling are required to accommodate such shortening. (See tomographic images in Fig. 3.) Using the VoiLA-P19 model (Braszus et al., 2021) for the same analysis does not change the results (Supplementary Fig.1).

transport has continued to at least 30 Ma and probably to the present-day, at a rate of 1 cm/yr with the North American plate. The offsets between the present and reconstructed subduction positions of R1 and R2 can be explained kinematically in a straightforward fashion by simply invoking the northwest movement of the entire Lesser Antilles slab with North America after subduction (Fig 8.d & f).

We explain the lateral offsets implied by our reconstruction by up to ~900 km WNW lateral transport of the Lesser Antilles slab within the mantle since 50 Ma (Fig. 8f). Indeed, a ~900 km WNW lateral offset between the 50 Ma and present (0 Ma) subducted ridge location is reasonable because the Caribbean upper plate has been relatively stationary in a mantle reference since 50 Ma whereas the Atlantic-North American lower plate has been moving WNW-wards during the same time frame (Fig. 1d). A recent study finds paleomagnetic evidence of differential block rotations and intra-plate shortening within the NE Caribbean (Montheil et al., 2023). These may imply additional eastward motion of the Caribbean plate interior 250- 500 km relative to North America since 50 Ma, depending on whether or not bookshelf-style rotation of near plate-boundary blocks is considered (Montheil et al., 2023). Accounting for the 250–500 km additional eastward Caribbean plate motion would delay the subduction history mentioned above by 5–10 or 10–15 Ma due to the more westward Lesser Antilles trench location. For the maximum motion, this would reduce our reconstructed distance of lateral slab transport to ~700 km during a 40 Myr subduction time interval, i.e. still implying substantial lateral slab transport.

5.2. Comparison to Lesser Antilles vertical slab sinking models

Our proposed ~900 km lateral transport of the Lesser Antilles slab, contrasts with the previous interpretation of a mainly vertically sinking slab in the Caribbean mantle (Braszus et al., 2021). Fig. 8e shows a comparison of our results against the purely 'vertical slab sinking' scenario. If the slab's sinking trajectory was mainly vertical, paleo-trench locations can be simply projected downwards from the Earth surface to the mantle (e.g., Figs. 8e & g). With this assumption, the position of R2 at the 50 Ma Lesser Antilles paleo-trench projects downwards to the slow-wavespeed slab anomaly A1 in our mapping; likewise, the 30 Ma position of R1 at the paleo-trench projects downwards to the slow wavespeed feature A0 in our mapping (Fig. 8e). Indeed, Braszus et al. (2021) associated R1 with A0 and R2 (subducted ~50 Ma) with A1 (Fig. 8e). Instead, here we associate R1 (subducted ~ 30 Ma) with A1 and R2 with A2 (Fig. 8d). In short, our work confirms the interpretation that these slow-wavespeed features correspond to subducted ridge segments (Braszus et al., 2021), but the ages of subduction are different from the predictions of the vertical sinking slab scenario.

Considering that the original separation between R1 and R2 in the reconstruction is ~900 km (Figs. 6e & 6f), a vertically sinking slab requires a 2–3 fold buckling of the slab to accommodate the shortening needed to achieve the ~350 km separation between A0 and A1in the present slab geometry (Fig. 8e,g). In contrast, lateral slab transport explains the similar separation between R1 and R2 in the reconstruction (Figs. 6e & 6f), and the separation between A1 and A2 in the present mantle (Figs. 8d, f); no significant slab buckling is required in this case. The vertical slab-sinking reconstruction also requires an overall factor 2–3 thickening/folding of the upper-mantle slab (Fig. 9b) to reconcile the ~500 km present-day slab length (as measured in the left panels of Fig. 3 as the distance from the present trench to the 50 Ma trench projected onto the slab) with the 1100 km of Caribbean-Atlantic convergence that is constrained by Cayman trough opening since 50 Ma. Although tomographic resolution may allow some slab thickening, none of the three tomographic models show clear indications of the required factor 2–3 slab thickening apart from at the southern end of the slab (Figs. 3d, j, and p).

For the earlier subduction history before 50 Ma, previous studies

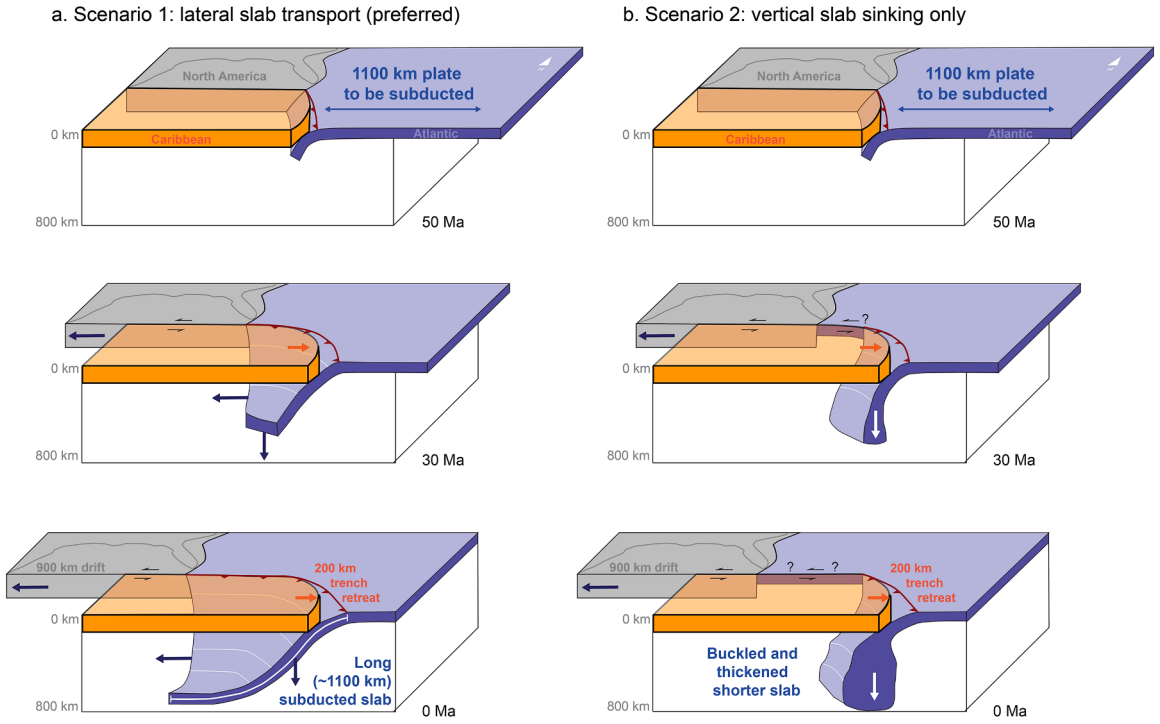

Fig. 9. Schematic block diagrams that show the two end-member scenarios for a Lesser Antilles slab to accommodate the convergence since 50 Ma. (a) In our preferred lateral slab transport scenario, the slab moves westwards laterally after subduction without significant internal deformation. This can maintain a slab geometry that shows a typical (~100 km) slab thickness and a slab length that is relatively comparable to the known Caribbean-North America plate convergence since 50 Ma (~1100 km). The proposed slab geometry is comparable to a cross-section in Fig. 2k. (b) In a vertical sinking scenario, the entire 1100 km plate convergence would be accommodated under a nearly fixed trench, which would imply a sub-vertical slab that would likely be thickening and buckling (e.g., Sigloch and Mihalynuk, 2013).

attributed lower-mantle high wavespeed anomalies below northeastern South America to subduction along the Greater Arc of the Caribbean since the mid-late Cretaceous (Braszus et al., 2021; van Benthem et al., 2013). These parts of the Proto-Caribbean slab are still best-explained if they sank approximately vertically (Braszus et al., 2021), although we acknowledge that uncertainties in the mantle reference frame in the Cretaceous and early Cenozoic (Müller et al., 1993; Müller et al., 2019; Torsvik et al., 2019) could complicate such interpretations.

The proposed change in the sinking behavior of the subducted slab coincides in time with a significant change in plate motions and in the configuration of subduction below the Caribbean plate (Müller et al., 2019; Braszus et al., 2021). Before ~65 Myr, the two Americas were moving apart, and active spreading in the Proto-Caribbean accommodated divergence (Müller et al., 2019; Pindell and Kennan, 2009). While Proto-Caribbean spreading was active (120–65 Ma), the GAC (the Greater Arc of the Caribbean) trench system migrated northwards with the two Americas in a mantle reference frame (Pindell et al., 2005). After 65Ma, the two Americas started to slowly converge, and Proto-Caribbean spreading stopped (Müller et al., 2019; Pindell and Kennan, 2009). Between 60–50 Myr, the western (Cuban) part of the GAC collided with the North American continental margin, and subduction ceased along this part of the arc (Pindell et al., 2005; Pindell and Kennan, 2009). Since 60–50 Ma, the motion of the Americas in a mantle reference frame has been mainly directed westward (Müller et al., 1993; Müller et al., 2019), and a new strike-slip plate boundary between the Caribbean and North America formed and opened the Cayman Trough (Mann et al., 2006; Pindell and Kennan, 2009). This change in plate motion and halt of subduction along the western part of the GAC could have induced significant shearing in the slab, possibly forcing detachment of what is currently the upper-mantle Lesser Antilles slab from the previously subducted sections of the slab now residing in the lower mantle. Our reconstruction suggests that the western edge of the Lesser Antilles slab could be a former fracture zone (Fig. 6e) that would localize such shearing and facilitate detachment from the older slab. Some of the older slabs had likely already reached the lower mantle, which would have increased resistance to lateral motion of the deeper slab to follow the surface plate motions (Billen, 2008; Čížková and Bina, 2013; Goes et al., 2017).

5.3. Significance of Lesser Antilles slab edges and the within-slab slow wavespeed anomalies

Like Braszus et al. (2021), our reconstruction highlights the tectonic importance of the fossil fracture zones and ridges within the Lesser Antilles slab (Fig. 7b). We suggest that slab edge 1 (labeled as green i in Fig. 7b) is a tear that developed along ridge segment, R2, (Fig. 7a) which stopped spreading only ~10 Myr before subducting (Braszus et al., 2021), while slab edge 2 (labeled as green ii in Fig. 7b) likely developed as the slab was torn along the former fracture zone directly west of R2 (the Caracas FZ in Fig. 7a). These interpretations are based on the unfolded slab edge locations that coincide with our reconstructed ridge and fracture zone positions (Figs. 6 & 7a). Slab tearing along edges 1 and 2 could have been induced by the changes in plate motion around 60–50 Ma that would have led to sheared detachment of the shallow from the deep slab, as discussed above. Slab edge 3 (labeled as green iii in Fig. 7b) corresponds to the southern edge of the Lesser Antilles slab, which was formed by a STEP fault type tear (Govers and Wortel, 2005) in the subducting plate forming the present strike-slip plate boundary at the El Pilar fault system near the South American continental margin (Fig. 1a).

Many of the wavespeed anomalies and edges of the Lesser Antilles slab thus follow pre-existing spreading ridges and fracture zones (Fig. 7a). Fracture zones have been considered weak zones on the oceanic lithosphere, especially when differently aged plates are juxtaposed, resulting in different negative buoyancies (Hensen et al., 2019). Major earthquakes that occurred along fracture zones on the Indian plate suggest that the mechanical strength of the oceanic lithosphere along these remains weak, e.g., due to fracturing and hydration, even after plate motion along them stops (e.g., Antolik et al., 2006; Hensen et al., 2019; Robinson et al., 2001). As noted previously, the spreading of the ridge segments (150–65 Ma) had already ceased by the time of their subduction in the Eocene. The reasons why fossil ridges serve as weak zones on the slab are likely due to their formation during a slow spreading (Müller et al., 2019), which in present-day examples is accommodated by > 50% tectonic accretion involving detachment faults and serpentinization (e.g., Escartín et al., 2008). The Atlantic lithosphere currently subducting below the Lesser Antilles Arc, which was formed at similar spreading rates as the Proto-Caribbean, is indeed substantially tectonized and serpentinized (Allen et al., 2022; Davy et al., 2020). Geochemical and geophysical observations around the present-day arc (Bie et al., 2019; Cooper et al., 2020; Hicks et al., 2023; Paulatto et al., 2017) are consistent with the subduction and dehydration of particularly serpentinized oceanic lithosphere below Dominica and Martinique, where we predict the location of subducted fossil ridge, R0 (Fig. 7b). Above R0 in the mantle wedge (Fig. 5c), the slow wavespeed body (Harmon et al., 2021) and enhanced seismic attenuation (Hicks et al., 2023) could be directly related to the dehydration of R0. We conclude that the main anomalies, gaps, and edges of the Lesser Antilles slab are inherited from pre-existing plate boundary structures in the subducted plate that were compositionally altered by hydration and remain weak.

Recent paleomagnetic data from the northern Antilles reveals significant block rotations of the arc implying up to 500 km westward motion of the Puerto-Rico-Virgin-Islands block since 40 Ma (Montheil et al., 2023). These rotations represent deformation of the upper plate, probably in response to the lateral motion of the slab we infer. Varying rotations along the arc (from north to south) indicate increasing oroclinal bending of the arc (Montheil et al., 2023). We suggest this arc bending allowed accommodating the different evolution of the northern and southern edges of the slab. The evolving STEP fault along the southern edge requires little evolution of arc curvature. However, in the north, the slab has remained connected to the surface plate, forcing increasing arc curvature as the leading edge of the slab moved westward.

5.4. Implications for slab strength and lateral slab transport

Slab motion is impeded by the highly viscous mantle (10^{19} - 10^{21} Pa s) around it, and the slab's own negative buoyancy only drives vertical sinking. To move the slab laterally, the attached surface plate must pull or push it, and stress needs to effectively transmit from the surface plate to the slab. Hence, lateral slab transport due to the subducted plate motion has been called ''slab dragging'' (Spakman et al., 2018).

Previous geodynamic models show that dragging a slab requires a strong slab whose effective viscosity is at least 2 orders of magnitude larger (10^{22} - 10^{24} Pa s) than the surrounding upper mantle (~10^{20} Pa s) (Chertova et al., 2014; Fraters et al., 2019). Such high slab viscosity is possible according to lab experiments (Billen and Hirth, 2007; Kohlstedt et al., 1995). However, geoid studies (Billen et al., 2003; Hager, 1984; Zhong and Davies, 1999), modeling of along-strike slab curvature (Loiselet et al., 2009), and downdip bending at the trench and near the base of the upper mantle (Buffett and Rowley, 2006; Čížková et al., 2002; Conrad and Hager, 1999) all suggest slabs are relatively weak while bending (only 1–2 orders of magnitude more viscous than the mantle).

Models that include composite nonlinear rheologies based on laboratory parameters show that such rheologies can reconcile the different strength estimates. Strain rate weakening in dislocation creep and yielding/plasticity substantially reduce the slab's resistance during bending, through strain localized at the top and bottom of the slab, while preserving a strong, high-viscosity core that is still able to transmit stresses (Buffett and Becker, 2012; Garel et al., 2014). With such rheologies, slab strength is recovered when strain rates are low (Billen and

Hirth, 2007; Garel et al., 2014), and models that incorporate such slabs show that by the base of the upper mantle, slab tips can be displaced by a few 100 to a 1000 km from where they subducted at the trench by drag/push from the subducting plate (Billen, 2008; Čížková and Bina, 2013; Goes et al., 2017). Some studies have suggested that additional weakening may be required to explain observed slab shapes, with a recent study showing that re-activation of subducted hydrated fractures could offer such a mechanism (Gerya et al., 2021). Dragging a slab in the direction of plate convergence tends to lead to increased slab bending and further weakening hinge at the trench (e.g., Fraters, 2019), while dragging opposite to convergence will decrease bending and hence increase its effective hinge strength. Effective slab viscosity will be relatively high when a slab is dragged parallel to its strike, in which direction weakening due to curvature is probably low.

Compared to other slabs that show significant lateral movements within the mantle) (Parsons et al., 2021; Qayyum et al., 2022; Spakman et al., 2018; Spakman and Hall, 2010; van de Lagemaat et al., 2018), the Lesser Antilles slab (Fig. 10) has been dragged over a similar distance (~1000 km) and at a moderate dragging velocity (~20 mm/yr). However, our results show that the Lesser Antilles slab experienced a longer duration of dragging (50 Myr) (Fig. 10). The currently subducting Atlantic lithosphere at the trench is relatively old (Fig. 6f) and hence strong at the trench compared to younger plates. However, the deeper slab appears torn along various pre-subduction plate weaknesses, such as fracture zones and spreading ridges. The observation that much of the drag occurred more or less along the strike of the northern part of the arc might explain how this slab could be dragged for close to 1000 km. Numerical experiments from Fraters (2019), who used a composite dislocation/diffusion/plastic slab rheology, show the plausibility of such drag and also show that even if there are gaps in the slab at the location of tomographic slow wavespeed anomalies, they do not strongly affect the dragging, as it is aided by the overall mantle flow pattern driven by the sinking slab and moving Americas. Other factors that may have facilitated/initiated the dragging of the slab subducted since 50 Ma could be (i) that the high strength of the old Atlantic lithosphere may preclude forming a STEP fault (Schliffke et al., 2022) which would be needed to allow migration of the northern tip of the Lesser Antilles Arc towards the Mid-Atlantic Ridge, instead forcing continued subduction below the Hispaniola-Virgin Island part of the trench that is now almost parallel to the direction of convergence, (ii) the relatively small size of the Lesser Antilles slab compared to the parent plates (North and South America), particularly if the deeper part of the slab had indeed been detached, may mean that strong driving forces are able to overcome dragging resistance (as in the models by Fraters (2019)). Several other slabs (e.g., the Gibraltar and the Banda slabs) that have been inferred to have been dragged were also small compared to the plates they were dragged by (Spakman et al., 2018; Spakman and Hall, 2010).

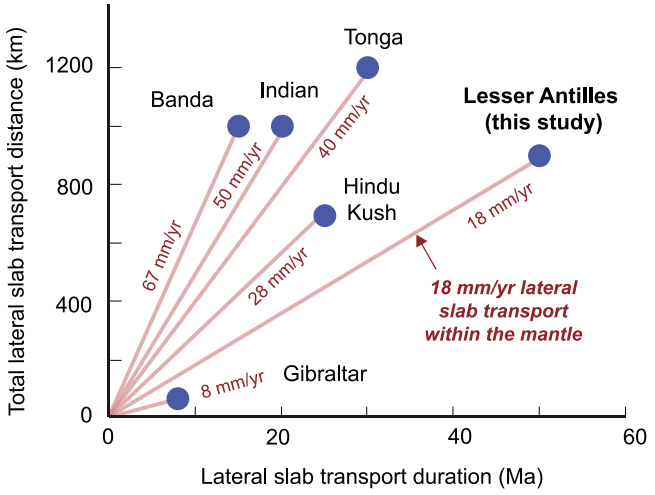

Fig. 10. Global compilation of laterally-transported slabs. The Lesser Antilles slab would have been transported laterally at a slow velocity of 18 mm/yr and over a moderate distance of 900 km compared to other cases of laterally-transported slabs (Tonga, van de Lagemaat et al., 2018; Gibraltar, Spakman et al., 2018; India, Parsons et al., 2021; Hindu Kush, Qayyum et al., 2022; Banda, Spakman and Hall, 2010).

6. Conclusion

We compared three published tomography models of the subducted slab underneath the eastern Caribbean, and we found that the three models consistently reveal a set of slow wavespeed anomalies within the upper-mantle slab. Based on our unfolded slab reconstruction, we interpret these reduced wavespeed zones as slab gaps/weakness zones along the fossil spreading ridges and fracture zones in the subducted plate, supporting previous results from Braszus et al. (2021). We found that the upper-mantle part of the slab accounts for subduction at the Lesser Antilles Arc from about 50 Ma, and that the current western edge of this slab likely formed as it tore along a fossil ridge and fracture zone, possibly in response to a plate motion change when the Cuban part of the Great Arc of the Caribbean (GAC) collided with the North American margin.

Our interpretations (Fig. 9) based on slab unfolding do not agree with the widely used assumption in comparing tomographic images and plate reconstructions that all slabs sink predominantly vertically at trenches. A previous interpretation assuming vertical sinking slab suggested the upper mantle Lesser Antilles slab represented about 70 Myr of subduction, requiring folding by 2–3 times its original thickness (Fig. 9b). Instead, our unfolded slab reconstruction suggests a relatively undeformed slab of which the tip was transported laterally by ~900 km after subduction (Fig. 9a). Such lateral transport in the mantle is likely due to the physical connection to the North American plate, whose northwestward motion since the Eocene has been dragging the slab in the same direction.

Lower mantle wavespeed anomalies that previous studies attributed to the earlier GAC subduction (Braszus et al., 2021; van Benthem et al., 2013) probably are still best explained by approximately vertical sinking. Our results strengthen previous suggestions that different modes of slab sinking are possible, where certain configurations of slab geometry and motion of the attached surface plates may allow for substantial lateral slab transport, placing them at distances as much as 1000 km from where they originally subducted. Our slab unfolding approach provides a new way to link mantle slabs to surface plate tectonics not requiring a-priori dynamic assumptions. Our work also shows the potential of analyzing the seismic wavespeed character of the unfolded slab to reconstruct fossil plate boundaries, which can be applied to other subduction zones.

Supplementary Figure 1. Sensitivity tests of our analysis using different tomography models. (a) and (b) are within-slab slow wavespeed anomalies in the present-day slab geometry with transferred wavespeeds from UUP07 (Amaru, 2007) and VoiLA-P19 (Braszus et al., 2021), respectively. The dashed lines show the locations of the slow wavespeed anomalies mapped from UUP07 model (same as Fig.8). For reference, we overlayed these dashed lines onto the slab with the wavespeeds of VoiLA-P19 superimposed. The hatched area in (b) reflects the bottom of the VoiLA-P19 model, as the model does not extend beyond 600 km depth (Braszus et al., 2021). (c) and (d) are the same analysis as Figs. 8a-c, but using slab surfaces with either the wavespeeds from UUP07 (Amaru, 2007) or VoiLA-P19 (Braszus et al., 2021) models. Although the relative amplitudes of the slab wavespeed anomalies are different between models, as expected due to different datasets and regularization in the inversions, the locations of the main anomalies and interpretations in terms of the amount of lateral slab transporting and deformation agree well

CRediT authorship contribution statement

Yi-Wei Chen: Writing – original draft, Visualization, Methodology, Investigation, Formal analysis, Conceptualization. **Jonny Wu:** Writing – review & editing, Supervision, Software, Methodology, Funding acquisition, Conceptualization. **Saskia Goes:** Writing – review & editing, Writing – original draft, Investigation.

Declaration of competing interest

The authors declare that they have no known competing financial interests or personal relationships that could have appeared to influence the work reported in this paper.

Data availability

The data used in this study has been published and can be freely obtained.

Acknowledgments

Y.W.C. and J.W. acknowledge support from US NSF Grant EAR-1848327 and funding provided to John Suppe through the University of Houston and the Governor's University Research Initiative (GURI) of the State of Texas. Y.W.C. acknowledge support from the German Research Foundation of the Research Training Group (UPLIFT) number 440512084. SG was supported by Natural Environment Research Council (NERC) grant NE/K010743/1 (VoiLA, Volatile Recycling in the Lesser Antilles). Educational licenses for the software Gocad were provided by Emerson Paradigm through the Paradigm University Program. We thank Dr. N. Harmon, Dr. C.W. Harris, and Dr. M. S. Miller for providing their tomography models. Paul Mann, John Suppe and Ray Russo are thanked for helpful discussions.

Supplementary materials

Supplementary material associated with this article can be found, in the online version, at doi:10.1016/j.epsl.2023.118561.

References

Allen, R.W., Collier, J.S., Henstock, T.J., Consortium, T.V., 2022. The Role of Crustal Accretion Variations in Determining Slab Hydration at an Atlantic Subduction Zone. J. Geophys. Res. 127, e2022JB024349.
Allen, R.W., Collier, J.S., Stewart, A.G., Henstock, T., Goes, S., Rietbrock, A., Team, t.V., 2019. The role of arc migration in the development of the Lesser Antilles: A new tectonic model for the Cenozoic evolution of the eastern Caribbean. Geology 47, 891–895.
Amaru, M., 2007. Global travel time tomography with 3-D reference models. Geologica Ultraiectina. Utrecht University, Utrecht, Netherlands.
Antolik, M., Abercrombie, R.E., Pan, J., Ekström, G., 2006. Rupture characteristics of the 2003 Mw 7.6 mid-Indian Ocean earthquake: Implications for seismic properties of young oceanic lithosphere. J. Geophys. Res. 111.
Bezada, M.J., Levander, A., Schmandt, B., 2010. Subduction in the southern Caribbean: Images from finite-frequency P wave tomography. J. Geophys. Res. 115.
Bie, L., Rietbrock, A., Hicks, S., Allen, R., Blundy, J., Clouard, V., Collier, J., Davidson, J., Garth, T., Goes, S., Harmon, N., Henstock, T., van Hunen, J., Kendall, M., Krüger, F., Lynch, L., Macpherson, C., Robertson, R., Rychert, K., Tait, S., Wilkinson, J., Wilson, M., 2019. Along-Arc Heterogeneity in Local Seismicity across the Lesser Antilles Subduction Zone from a Dense Ocean-Bottom Seismometer Network. Seismol. Res. Lett. 91, 237–247.
Billen, M.I., 2008. Modeling the Dynamics of Subducting Slabs. Annu. Rev. Earth Planet. Sci. 36, 325–356.
Billen, M.I., Gurnis, M., Simons, M., 2003. Multiscale dynamics of the Tonga—Kermadec subduction zone. Geophys. J. Int. 153, 359–388.
Billen, M.I., Hirth, G., 2007. Rheologic controls on slab dynamics. Geochemistry, Geophysics, Geosystems 8.
Bird, P., 2003. An updated digital model of plate boundaries. Geochem. Geophys. Geosyst. 4, 1027.
Braszus, B., Goes, S., Allen, R., Rietbrock, A., Collier, J., Harmon, N., Henstock, T., Hicks, S., Rychert, C.A., Maunder, B., van Hunen, J., Bie, L., Blundy, J., Cooper, G., Davy, R., Kendall, J.M., Macpherson, C., Wilkinson, J., Wilson, M., 2021. Subduction history of the Caribbean from upper-mantle seismic imaging and plate reconstruction. Nat. Commun. 12, 4211.
Brune, S., Heine, C., Pérez-Gussinyé, M., Sobolev, S.V., 2014. Rift migration explains continental margin asymmetry and crustal hyper-extension. Nat. Commun. 5, 4014.
Buffett, B.A., Becker, T.W., 2012. Bending stress and dissipation in subducted lithosphere. J. Geophys. Res. 117.
Buffett, B.A., Rowley, D.B., 2006. Plate bending at subduction zones: Consequences for the direction of plate motions. Earth Planet. Sci. Lett. 245, 359–364.
Cediel, F., 2019. Phanerozoic Orogens of Northwestern South America: Cordilleran-Type Orogens. Taphrogenic Tectonics. The Maracaibo Orogenic Float. The Chocó-Panamá Indenter. In: Cediel, F., Shaw, R.P. (Eds.), Geology and Tectonics of Northwestern South America: The Pacific-Caribbean-Andean Junction. Springer International Publishing, Cham, pp. 3–95.
Chen, Y.W., Wu, J., Suppe, J., 2019. Southward propagation of Nazca subduction along the Andes. Nature 565, 441–447.
Chertova, M.V., Spakman, W., van den Berg, A.P., van Hinsbergen, D.J.J., 2014. Absolute plate motions and regional subduction evolution. Geochem. Geophys. Geosyst. 15, 3780–3792.
Čížková, H., Bina, C.R., 2013. Effects of mantle and subduction-interface rheologies on slab stagnation and trench rollback. Earth Planet. Sci. Lett. 379, 95–103.
Čížková, H., van Hunen, J., van den Berg, A.P., Vlaar, N.J., 2002. The influence of rheological weakening and yield stress on the interaction of slabs with the 670 km discontinuity. Earth Planet. Sci. Lett. 199, 447–457.
Conrad, C.P., Hager, B.H., 1999. Effects of plate bending and fault strength at subduction zones on plate dynamics. J. Geophys. Res. 104, 17551–17571.
Cooper, G.F., Macpherson, C.G., Blundy, J.D., Maunder, B., Allen, R.W., Goes, S., Collier, J.S., Bie, L., Harmon, N., Hicks, S.P., Iveson, A.A., Prytulak, J., Rietbrock, A., Rychert, C.A., Davidson, J.P., Cooper, G.F., Macpherson, C.G., Blundy, J.D., Maunder, B., Allen, R.W., Goes, S., Collier, J.S., Bie, L., Harmon, N., Hicks, S.P., Rietbrock, A., Rychert, C.A., Davidson, J.P., Davy, R.G., Henstock, T.J., Kendall, M. J., Schlaphorst, D., van Hunen, J., Wilkinson, J.J., Wilson, M., the Voi, L.A.t., 2020. Variable water input controls evolution of the Lesser Antilles volcanic arc. Nature 582, 525–529.
Davy, R.G., Collier, J.S., Henstock, T.J., Consortium, T.V., 2020. Wide-Angle Seismic Imaging of Two Modes of Crustal Accretion in Mature Atlantic Ocean Crust. J. Geophys. Res. 125, e2019JB019100.
Dziewonski, A.M., Chou, T.A., Woodhouse, J.H., 1981. Determination of earthquake source parameters from waveform data for studies of global and regional seismicity. J. Geophys. Res. 86, 2825–2852.
Ekström, G., Nettles, M., Dziewoński, A.M., 2012. The global CMT project 2004–2010: Centroid-moment tensors for 13,017 earthquakes. Phys. Earth Planet. Inter. 200-201, 1–9.
Engdahl, E.R., Villaseñor, A., 2002. 41 Global seismicity: 1900–1999. Mar. Geol. 81, 665–XVI.
Escartín, J., Smith, D.K., Cann, J., Schouten, H., Langmuir, C.H., Escrig, S., 2008. Central role of detachment faults in accretion of slow-spreading oceanic lithosphere. Nature 455, 790–794.
Fraters, M., 2019. Towards Numerical Modelling of Natural Subduction Systems With an Application to Eastern Caribbean Subduction. Earth Sciences. Utrecht University.
Fraters, M., Spakman, W., Thieulot, C., Van Hinsbergen, D.J., 2019. Assessing the geodynamics of strongly arcuate subduction zones in the eastern Caribbean subduction setting. In: AGU Fall Meeting Abstracts, pp. T23A–T207.
Garel, F., Goes, S., Davies, D.R., Davies, J.H., Kramer, S.C., Wilson, C.R., 2014. Interaction of subducted slabs with the mantle transition-zone: A regime diagram from 2-D thermo-mechanical models with a mobile trench and an overriding plate. Geochem. Geophys. Geosyst. 15, 1739–1765.
Gerya, T.V., Bercovici, D., Becker, T.W., 2021. Dynamic slab segmentation due to brittle–ductile damage in the outer rise. Nature 599, 245–250.
Goes, S., Agrusta, R., van Hunen, J., Garel, F., 2017. Subduction-transition zone interaction: A review. Geosphere 13, 644–664.
Goes, S., Collier, J., Blundy, J., Davidson, J., Harmon, N., Henstock, T., Kendall, J., Macpherson, C., Rietbrock, A., Rychert, K., Prytulak, J., van Hunen, J., Wilkinson, J., Wilson, M., 2019. Project VoiLA: Volatile Recycling in the Lesser Antilles. Trans. Am. Geophys. Union 100.
Govers, R., Wortel, M.J.R., 2005. Lithosphere tearing at STEP faults: response to edges of subduction zones. Earth Planet. Sci. Lett. 236, 505–523.
Hager, B., 1984. Subducted Slabs and the Geoid: Constraints on Mantle Rheology and Flow. J. Geophys. Res. 89.
Harmon, N., Rychert, C.A., Goes, S., Maunder, B., Collier, J., Henstock, T., Lynch, L., Rietbrock, A., Group, t.V.W., 2021. Widespread Hydration of the Back Arc and the Link to Variable Hydration of the Incoming Plate in the Lesser Antilles From Rayleigh Wave Imaging. Geochem. Geophys. Geosyst. 22, e2021GC009707.
Harris, C.W., Miller, M.S., Porritt, R.W., 2018. Tomographic Imaging of Slab Segmentation and Deformation in the Greater Antilles. Geochem. Geophys. Geosyst. 19, 2292–2307.
Hensen, C., Duarte, J.C., Vannucchi, P., Mazzini, A., Lever, M.A., Terrinha, P., Géli, L., Henry, P., Villinger, H., Morgan, J., Schmidt, M., Gutscher, M.A., Bartolome, R., Tomonaga, Y., Polonia, A., Gràcia, E., Tinivella, U., Lupi, M., Çağatay, M.N., Elvert, M., Sakellariou, D., Matias, L., Kipfer, R., Karageorgis, A.P., Ruffine, L., Liebetrau, V., Pierre, C., Schmidt, C., Batista, L., Gasperini, L., Burwicz, E., Neres, M., Nuzzo, M., 2019. Marine Transform Faults and Fracture Zones: A Joint Perspective Integrating Seismicity, Fluid Flow and Life. New Front. Rare Earth Sci. Appl. Proc. Int. Conf. Rare Earth Dev. Appl. 7.
Hicks, S.P., Bie, L., Rychert, C.A., Harmon, N., Goes, S., Rietbrock, A., Wei, S.S., Collier, J.S., Henstock, T.J., Lynch, L., Prytulak, J., Macpherson, C.G., Schlaphorst, D., Wilkinson, J.J., Blundy, J.D., Cooper, G.F., Davy, R.G., Kendall, J.

M., Group, V.W., 2023. Slab to back-arc to arc: Fluid and melt pathways through the mantle wedge beneath the Lesser Antilles. Sci. Adv. 9, eadd2143.
Kohlstedt, D.L., Evans, B., Mackwell, S.J., 1995. Strength of the lithosphere: Constraints imposed by laboratory experiments. J. Geophys. Res. 100, 17587–17602.
Levander, A., Bezada, M.J., Niu, F., Humphreys, E.D., Palomeras, I., Thurner, S.M., Masy, J., Schmitz, M., Gallart, J., Carbonell, R., Miller, M.S., 2014. Subduction-driven recycling of continental margin lithosphere. Nature 515, 253–256.
Lindner, M., Rietbrock, A., Bie, L., Goes, S., Collier, J., Rychert, C., Harmon, N., Hicks, S. P., Henstock, T., group, t.V.w.,, 2023. Bayesian regional moment tensor from ocean bottom seismograms recorded in the Lesser Antilles: implications for regional stress field. Geophys. J. Int. 233, 1036–1054.
Loiselet, C., Husson, L., Braun, J., 2009. From longitudinal slab curvature to slab rheology. Geology 37, 747–750.
Macdonald, K.C., 1998. Linkages Between Faulting, Volcanism, Hydrothermal Activity and Segmentation on Fast Spreading Centers. Faulting and Magmatism at Mid-Ocean Ridges 27–58.
Mann, P., Rogers, R.D., Gahagan, L., 2006. Overview of plate tectonic history and its unresolved tectonic problems. In: Bundschuh, J.A., G, E. (Eds.), Central America: Geology, Resources and Hazards, pp. 201–237.
Masy, J., Niu, F., Levander, A., Schmitz, M., 2015. Lithospheric expression of cenozoic subduction, mesozoic rifting and the Precambrian Shield in Venezuela. Earth Planet. Sci. Lett. 410, 12–24.
Meighan, H.E., Pulliam, J., 2013. Seismic anisotropy beneath the northeastern Caribbean: Implications for the subducting North American lithosphere. Bulletin de la Société Géologique de France 184, 67–76.
Miller, M.S., Levander, A., Niu, F., Li, A., 2009. Upper mantle structure beneath the Caribbean-South American plate boundary from surface wave tomography. J. Geophys. Res. 114.
Montheil, L., Philippon, M., Münch, P., Camps, P., Vaes, B., Cornée, J.J., Poidras, T., van Hinsbergen, D.J.J., 2023. Paleomagnetic Rotations in the Northeastern Caribbean Region Reveal Major Intraplate Deformation Since the Eocene. Tectonics 42, e2022TC007706.
Müller, R.D., Royer, J.Y., Lawver, L.A., 1993. Revised plate motions relative to the hotspots from combined Atlantic and Indian Ocean hotspot tracks. Geology 21, 275–278.
Müller, R.D., Zahirovic, S., Williams, S.E., Cannon, J., Seton, M., Bower, D.J., Tetley, M. G., Heine, C., Le Breton, E., Liu, S., Russell, S.H.J., Yang, T., Leonard, J., Gurnis, M., 2019. A Global Plate Model Including Lithospheric Deformation Along Major Rifts and Orogens Since the Triassic. Tectonics 38, 1884–1907.
Parsons, A.J., Sigloch, K., Hosseini, K., 2021. Australian Plate Subduction is Responsible for Northward Motion of the India-Asia Collision Zone and ~1,000 km Lateral Migration of the Indian Slab. Geophys. Res. Lett. 48, e2021GL094904.
Paulatto, M., Laigle, M., Galve, A., Charvis, P., Sapin, M., Bayrakci, G., Evain, M., Kopp, H., 2017. Dehydration of subducting slow-spread oceanic lithosphere in the Lesser Antilles. Nat. Commun. 8, 15980.
Pavlis, T.L., Amato, J.M., Trop, J., Ridgway, K., Roeske, S., Gehrels, G., 2019. Subduction polarity in ancient arcs: A call to integrate geology and geophysics to decipher the Mesozoic tectonic history of the Northern Cordillera of North America. GSA Today 29, 4–10.
Peng, D., Liu, L., 2022. Quantifying slab sinking rates using global geodynamic models with data-assimilation. Earth Sci. Rev. 230, 104039.
Pindell, J., Kennan, L., Maresch, W.V., Stanek, K.P., Draper, G., Higgs, R., Lallemant, H. G.A., Sisson, V.B., 2005. Plate-kinematics and Crustal Dynamics of Circum-Caribbean Arc-Continent interactions: Tectonic controls On Basin Development in Proto-Caribbean margins, Caribbean-South American Plate Interactions. Geological Society of America, Venezuela, p. 0.
Pindell, J.L., Kennan, L., 2009. Tectonic evolution of the Gulf of Mexico, Caribbean and northern South America in the mantle reference frame: an update. In: Geological Society, 328. Special Publications, London, pp. 1–55.
Qayyum, A., Lom, N., Advokaat, E.L., Spakman, W., van der Meer, D.G., van Hinsbergen, D.J.J., 2022. Subduction and Slab Detachment Under Moving Trenches During Ongoing India-Asia Convergence. Geochem. Geophys. Geosyst. 23, e2022GC010336.
Ren, Y., Stutzmann, E., van der Hilst, R.D., Besse, J., 2007. Understanding seismic heterogeneities in the lower mantle beneath the Americas from seismic tomography and plate tectonic history. J. Geophys. Res. 112.
Robinson, D.P., Henry, C., Das, S., Woodhouse, J.H., 2001. Simultaneous Rupture Along Two Conjugate Planes of the Wharton Basin Earthquake. Science 292, 1145–1148.
Sandwell, D.T., Müller, R.D., Smith, W.H.F., Garcia, E., Francis, R., 2014. New global marine gravity model from CryoSat-2 and Jason-1 reveals buried tectonic structure. Science 346, 65–67.
Schlaphorst, D., Kendall, J.M., Baptie, B., Latchman, J.L., Tait, S., 2017. Gaps, tears and seismic anisotropy around the subducting slabs of the Antilles. Tectonophysics 698, 65–78.
Schliffke, N., van Hunen, J., Allen, M.B., Magni, V., Gueydan, F., 2022. Episodic back-arc spreading centre jumps controlled by transform fault to overriding plate strength ratio. Nat. Commun. 13, 582.
Schmitz, M., Ramírez, K., Mazuera, F., Ávila, J., Yegres, L., Bezada, M., Levander, A., 2021. Moho depth map of northern Venezuela based on wide-angle seismic studies. J. South Amer. Earth Sci. 107, 103088.
Sigloch, K., Mihalynuk, M.G., 2013. Intra-oceanic subduction shaped the assembly of Cordilleran North America. Nature 496, 50–56.
Sigloch, K., Mihalynuk, M.G., 2017. Mantle and geological evidence for a Late Jurassic–Cretaceous suture spanning North America. Geol. Soc. Am. Bull. 129, 1489–1520.
Spakman, W., Chertova, M.V., van den Berg, A., van Hinsbergen, D.J.J., 2018. Puzzling features of western Mediterranean tectonics explainedby slab dragging. Nat. Geosci. 11, 211–216.
Spakman, W., Hall, R., 2010. Surface deformation and slab–mantle interaction during Banda arc subduction rollback. Nat. Geosci. 3, 562–566.
Torsvik, T.H., Steinberger, B., Shephard, G.E., Doubrovine, P.V., Gaina, C., Domeier, M., Conrad, C.P., Sager, W.W., 2019. Pacific-Panthalassic Reconstructions: Overview, Errata and the Way Forward. Geochem. Geophys. Geosyst. 20, 3659–3689.
Trude, J., Kilsdonk, B., Grow, T., Ott, B., 2022. The structure and tectonics of the Guyana Basin. In: Geological Society, 524. Special Publications, London. SP524-2021-2117.
van Benthem, S., Govers, R., Spakman, W., Wortel, R., 2013. Tectonic evolution and mantle structure of the Caribbean. J. Geophys. Res. 118, 3019–3036.
van de Lagemaat, S.H.A., van Hinsbergen, D.J.J., Boschman, L.M., Kamp, P.J.J., Spakman, W., 2018. Southwest Pacific Absolute Plate Kinematic Reconstruction Reveals Major Cenozoic Tonga-Kermadec Slab Dragging. Tectonics 37, 2647–2674.
van der Hilst, R.D., Widiyantoro, S., Engdahl, E.R., 1997. Evidence for deep mantle circulation from global tomography. Nature 386, 578–584.
van der Meer, D.G., van Hinsbergen, D.J.J., Spakman, W., 2018. Atlas of the underworld: Slab remnants in the mantle, their sinking history, and a new outlook on lower mantle viscosity. Tectonophysics 723, 309–448.
VanDecar, J.C., Russo, R.M., James, D.E., Ambeh, W.B., Franke, M., 2003. Aseismic continuation of the Lesser Antilles slab beneath continental South America. J. Geophys. Res. 108.
Whattam, S.A., Stern, R.J., 2015. Late Cretaceous plume-induced subduction initiation along the southern margin of the Caribbean and NW South America: The first documented example with implications for the onset of plate tectonics. Gondwana Res. 27, 38–63.
Wu, J., Suppe, J., Lu, R., Kanda, R., 2016. Philippine Sea and East Asian plate tectonics since 52 Ma constrained by new subducted slab reconstruction methods. J Geophys Res 121, 4670–4741.
Zhong, S., Davies, G.F., 1999. Effects of plate and slab viscosities on the geoid. Earth Planet. Sci. Lett. 170, 487–496.